Virus Research 265 (2019) 47–56

Contents lists available at ScienceDirect

Virus Research

journal homepage: www.elsevier.com/locate/virusres

Porcine reproductive and respiratory syndrome virus (PRRSV)-induced stress granules are associated with viral replication complexes and suppression of host translation

Nicholas Catanzaro, Xiang-Jin Meng*

Department of Biomedical Sciences and Pathobiology, Virginia-Maryland College of Veterinary Medicine, Virginia Polytechnic Institute and State University, Blacksburg, VA, USA

ARTICLE INFO

Keywords:
Porcine reproductive and respiratory syndrome virus (PRRSV)
Stress granule (SG)
Protein translation
Stress response

ABSTRACT

Stress granules (SGs) are dynamic sites of cytosolic mRNA storage that are formed in response to stress conditions, including viral infection. SGs have been implicated in regulating several aspects of the host immune response to various pathogens. Porcine reproductive and respiratory syndrome virus (PRRSV), an economically-important global swine pathogen, reportedly induced SGs during replication, although the underlying mechanisms are poorly defined. In this study, we delineated the molecular mechanisms regulating the SG response to PRRSV infection. Using confocal microscopy, we first demonstrated that infection with PRRSV strain VR2385 induces an accumulation of the SG markers G3BP1, G3BP2, TIAR, eIF3b, and USP10 as well as mRNAs into punctate structures in the cytoplasm of infected host cells. Subsequently, we demonstrated that the PRRSV-induced SGs were in close proximity to viral replication complexes (VRCs) and processing bodies (P-bodies), and that SG formation was coordinated with inhibition of host cellular translation. Treatment of infected cells with cycloheximide disrupted the PRRSV-induced SGs. Furthermore, impairment of SG assembly by the shRNA-mediated knockdown of G3BP1, G3BP2 and USP10 did not affect viral replication. Collectively, these results demonstrate that PRRSV infection induces formation of SGs associated with VRCs, which is coordinated with the suppression of host cell protein synthesis. This is the first study to extensively characterize the formation and underlying mechanism of *bona fide* SGs during PRRSV infection. Our findings have important implications in understanding the mechanism of PRRSV-host interactions.

1. Introduction

Porcine reproductive and respiratory syndrome (PRRS) is inarguably the most economically devastating disease affecting the global swine industry. The disease is typically characterized by reproductive failures in pregnant sows and acute respiratory disease in young piglets (Lunney et al., 2010). In the United States alone, PRRS is estimated to cause more than $600 million in production losses each year (Neumann et al., 2005; Holtkamp et al., 2013). The causative agent of the disease, PRRS virus (PRRSV), was identified and characterized first in the Netherlands (Meulenberg et al., 1993) and subsequently in the United States (Collins et al., 1992; Snijder et al., 2013). Following the acute phase of infection, PRRSV can establish a persistent infection lasting for several months. Persistently-infected animals continuously shed virus and are therefore important sources of transmission to naïve pigs within the herd (Snijder et al., 2013). PRRSV infection suppresses all facets of the host's immune response, characterized by weak cellular and humoral immune responses that are suboptimal compared to other swine pathogens. PRRSV is also a poor inducer of the antiviral type I interferons (IFNs), important cytokines that bridge the innate and adaptive immune responses (Sun et al., 2012a). Due to the extensive genetic diversity of PRRSV, current available vaccines only offer limited protection to heterologous strains (Ke and Yoo, 2017; Renukaradhya et al., 2015). Only with a better understanding of the molecular mechanisms of PRRSV immune evasion will we be able to design more effective vaccines.

PRRSV is a single-stranded, positive-sense enveloped RNA virus in the family *Arteriviridae* of the order *Nidovirales* (Meng et al., 1994,

Abbreviations: VRCs, viral replication complexes; P-bodies, processing bodies; G3BP1, G3BP stress granule assembly factor 1; G3BP2, G3BP stress granule assembly factor 2; TIAR, T-cell-restricted intracellular antigen proteins; eIF3b, eukaryotic translation initiation factor 3 subunit B; eIF2a, alpha subunit of eukaryotic initiation factor 2; USP10, ubiquitin specific peptidase 10; PICs, pre-initiations complexes; RBPs, RNA-binding proteins

* Corresponding author at: College of Veterinary Medicine, Virginia Tech, 1981 Kraft Drive, Blacksburg, VA, 24061-0913, USA.
E-mail address: xjmeng@vt.edu (X.-J. Meng).

https://doi.org/10.1016/j.virusres.2019.02.016
Received 13 December 2018; Received in revised form 20 February 2019; Accepted 27 February 2019
Available online 01 March 2019
0168-1702/

1996). The PRRSV genome is approximately 15 kb in length and contains eleven known open reading frames (ORFs) (Snijder et al., 2013). The 3′ end of the genome encodes structural proteins GP2a, GP3, GP4 GP5, GP5a, M and N. The replication-associated genes, ORF1a and ORF1b, are located at the 5′ end of the genome and encode two large polyproteins, pp1a and pp1b, respectively (Snijder et al., 2013; Fang and Snijder, 2010). A proteolytic cascade mediated by four proteinase domains encoded in the ORF1a processes the polyproteins into 14 nonstructural proteins (NSPs) (Fang and Snijder, 2010). Of the NSPs, NSP1α, NSP1β, and NSP2 have been shown to strongly antagonize the type I IFN response (Beura et al., 2010, 2012; Sun et al., 2012b), although the molecular mechanisms responsible for this inhibition are not completely understood (Sun et al., 2012a).

Stress granules (SGs) are dynamic cytoplasmic protein-RNA structures that quickly form and dissolve in response to various stress conditions (Panas et al., 2016). Heat shock, oxidative stress, and viral infection have all been shown to induce robust SG formation in various cell types (Taniuchi et al., 2016). Cellular kinases respond to these stresses by phosphorylating the alpha subunit of eukaryotic initiation factor 2 (eIF2a). As a result, the available eIF2/tRNAiMet/GTP ternary complex is depleted. A reduction in this complex results in the reversible inhibition of translation and subsequent polysome disassembly accumulation of stalled 43S and 48S ribosomal pre-initiations complexes (PICs). Stalled PICs in turn recruit RNA-binding proteins (RBPs) such as G3BP1, G3BP2, TIAR and other proteins that are involved in SG nucleation (Panas et al., 2016; Kedersha et al., 1999). A hallmark feature of canonical, *bona fide* SGs is the presence of these protein factors along with mRNAs (Panas et al., 2015; Lloyd, 2012). SGs are thought to associate with another cellular mRNA repository known as a processing body (P-body). While SGs are temporary storage sites of mRNA during cellular stress, P-bodies are thought to specifically act as sites of mRNA degradation in cells. It is currently thought that mRNAs are transiently stored in SGs until they are either released for translation, or transferred to P-bodies for degradation (Panas et al., 2016; Mollet et al., 2008; Brengues et al., 2005). Formation of SGs and P-bodies in cells are directly involved in global repression of specific host mRNAs (Panas et al., 2016).

PRRSV reportedly induced SGs during infection to regulate the antiviral response (Zhou et al., 2017), although the underlying mechanism is not fully understood. Here, we first definitively demonstrated that PRRSV infection induces *bona fide* SGs, although they differ from the canonical SGs in terms of size and distribution. These granules are closely associated with viral replication complexes (VRCs) and P-bodies, and their formation is coordinated with the phosphorylation of eIF2a and subsequent arrest in cellular translation. The PRRSV-induced SGs were disrupted upon cycloheximide treatment. Ablation of the PRRSV-induced granules through the shRNA silencing of G3BP1 and G3BP2 had no effect on viral replication. Collectively, our results indicate that PRRSV-induced SGs are involved in, but not required, for efficient viral replication. However, the role of SGs in regulating the immune response to PRRSV still warrants further investigation in the future.

2. Materials and methods

2.1. Cells, viruses and chemicals

BHK-21 cells were cultured in Dulbecco's Modified Eagle Medium (DMEM, Invitrogen) supplemented with 10% fetal bovine serum (FBS, Invitrogen). The PRRSV-susceptible monkey kidney cell line, MARC-145, was cultured and maintained in DMEM supplemented with 10% FBS. The porcine kidney cell line, PK-15, was made susceptible to PRRSV infection by overexpressing the PRRSV receptor, CD163. The PK-15^{CD163} cells were maintained in MEM supplemented with 10% FBS. The PRRSV strain VR2385 used in this study was originally isolated from a pig with severe PRRS in Iowa (Meng et al., 1994). The PRRSV VR2385 virus stock was produced by transfection of BHK-21 cells with the PRRSV VR2385 infectious cDNA clone plasmid (pIR-VR2385-EGFP) (Ni et al., 2011). Sodium arsenite (SA) (Sigma) was used as positive control to induced SG formation. Cycloheximide (CHX, Sigma) was used to disrupt both SA- and PRRSV-induced SGs.

2.2. Immunofluorescence staining and confocal microscopy

For immunofluorescence (IFA) microscopy, cells were grown on glass coverslips in 6-well plates. At the indicated times post-treatment, cells were fixed with 4% paraformaldehyde in PBS for 15 min at room temperature. Cells were then blocked and permeabilized in 10% normal goat serum and 0.3% triton-x 100 in PBS for 1 h at room temperature, followed by incubation with respective primary antibodies with 5% normal goat serum in PBS for 16 h at 4 °C. Cells were then washed three times with PBS and incubated with secondary antibodies in 5% normal goat serum in PBS at room temperature for 2 h. Nuclei were stained with DAPI and cells were washed three times prior to being mounted on glass slides with Aquapolymount. Fluorescent images were examined using a confocal laser scanning microscope (LSM880, Carl Zeiss). The antibodies used for IFA confocal microscopy were as follows: rabbit anti-eIF3b (Bethyl), rabbit anti-TIAR (Bethyl), rabbit anti-G3BP1 (Bethyl), mouse anti-G3BP1 (Santa Cruz), rabbit anti-G3BP2 (Bethyl), mouse anti-dsRNA (Scicons), rabbit anti-Dcp1a (Bethyl), mouse anti-puromycin (Millipore), goat anti-mouse conjugated to Alexa546 (Thermo), and goat anti-rabbit conjugated to Alexa647 (Thermo).

2.3. Quantification of SG-positive cells

Cells were considered SG positive if they contained 3 or more SG marker foci (Panas et al., 2015). At least 100 cells were counted for each of the SG markers indicated in randomly selected fields of view.

2.4. Western blot analysis and quantification

Cells were lysed in RIPA lysis buffer, centrifuged at 14,000 rpm for 10 min at 4 °C, and then diluted in 1:4 in 4X Laemmli sample buffer. Equal amounts of proteinwere resolved using a 4–20% gradient gel and transferred to PVDF membrane. Membranes were subsequently blocked for 1 h at room temperature using Odyssey TBS Blocking Buffer (Licor), and incubated with primary antibodies diluted in Odyssey TBS Blocking Buffer containing 0.1% tween 20 for 16 h at 4C. Membranes were washed three times with TBS-T (0.1% tween 20) and then incubated with secondary antibodies diluted in Odyssey Blocking Buffer containing 0.1% tween 20. After washing three times with TBS-T (0.1% tween 20), the membranes were then imaged using a LicorClx Imaging System. Western blot band intensities were quantified using Licor Image Studio Software. The antibodies used for western blot analysis are the same as used in IFA confocal microscopy experiments described above, with the addition of rabbit anti-phospho eIF2a, rabbit anti-total eIF2a, mouse anti-GAPDH (Thermo), rabbit anti-NSP2, goat anti-rabbit conjugated to IRDye680 (Licor) and goat anti-mouse conjugated to IRDye800 (Licor).

2.5. Fluorescent in situ hybridization (FISH) assay

FISH assays were performed as described previously (Park et al., 2008). Briefly, cells were fixed and stained as described above for IFA confocal microscopy. After the final incubation with secondary antibodies, coverslips were incubated with for 16 hous at 4 °C with oligodT (Reid et al., 2015) conjugated to Alexa647 diluted in FISH Buffer (2X SSC, 20% formamide, 0.2% bovine serum albumin, 1 μg yeast tRNA/μl,). The next day, nuclei were stained with DAPI and cells were washed three times prior to being mounted on glass slides with Aquapolymount. Cells were then examined using confocal microscopy as described above.

2.6. Puromycylation assay

Puromycin incorporation assay was performed as described previously (Panas et al., 2015). Briefly, MARC-145 cells were treated with 10 μg/mL puromycin for 15 min at 37C prior to fixation. Cells were then analyzed using confocal microscopy as described above.

2.7. G3BP1, G3BP2 and USP10 shRNA knockdown

Lentiviral particles were generated via transfection of HEK293 T cells in T25 flasks with 1.875 μg psPAX, 0.625 μg pMD2.G, and 2.5 μg of the pLKO.1 construct expressing shRNA against G3BP1 (TRCN0000008719), G3BP2 (TRCN0000047548) and USP10 (V2LHS_254993) or the empty pLKO.1 vector negative control expressing an 18 bp stuffer sequence (Dharmacon). At 48 h post-transduction, culture supernatant was harvested and used to transduce MARC-145 cells. Stably-transduced cells were selected in 5 μg/mL puromycin for 72 h. Knockdown efficiency was determined via western blot analysis as described above.

2.8. Plaque assays

Plaque assays were performed as previously described (Ni et al., 2011). Briefly, plaque assays were performed in triplicate on supernatants from MARC-145 cells infected with PRRSV at the indicated times post-infection. Plaques were allowed to develop for 72 h before being stained with 1% crystal violet and counted.

3. Results

3.1. PRRSV infection induces SGs

Considering the dichotomous nature of SGs in virus-induced stress responses, we further investigated SG formation in response to PRRSV infection. Here, we infected the PRRSV-permissive monkey kidney cell line, MARC-145, with a highly virulent strain of PRRSV (strain VR2385-EGFP) and analyzed the distribution of G3BP1 at 48 h post-infection (hpi). G3BP1 is an RNA-binding protein that exhibits both endoribonuclease and helicase activities, and is also a regulator of SG assembly that is commonly used as a SG marker (Tourrière et al., 2003). G3BP1 and other SG markers are constitutively expressed under homeostatic conditions within the cell. Upon stress, markers form cytoplasmic foci, collectively referred to as SGs. In this paper, SG positive cells are defined by the presence of 3 or more cytoplasmic foci of any given SG marker. In mock-infected cells, G3BP1 was diffusely distributed throughout the cytoplasm. As a positive control, cells treated with sodium arsenite (SA), a previously established SG inducer (Panas et al., 2015), were shown to form robust SGs as indicated by the presence of G3BP1 positive cytoplasmic punctate foci. PRRSV-infected cells were identified by the presence of NSP2-EGFP. Similar to the SA treated cells, PRRSV infected cells also exhibited a SG response (Fig.1A). Compared to the mock infected cells, the number of SA-treated and PRRSV-infected cells containing SGs was significantly higher as nearly 100% of cells counted at 48 hpi were SG-positive (Fig. 1B). Since SGs are transient in nature, we also examined earlier time points during PRRSV infection at 12, 24, 48 and 72 h (data not shown). We found that the PRRSV-induced SGs were only present during the 48–72 hour time points, suggesting the SG-response only occurs during the later stages of PRRSV infection. SGs are heterogeneous structures and depending on the initial stress condition, the protein and mRNA content is extremely variable (Aulas et al., 2017). To determine whether PRRSV-induced SGs contain additional typical SG marker proteins, we examined the distribution of the translation initiation factor eIF3b, and other RBPs including TIAR and G3BP2. The ubiquitin specific protease, USP10, was also examined (Supplemental Fig. S1). These proteins are considered markers of canonical SGs (Panas et al., 2015). Confocal microscopy revealed that eIF3b, TIAR, G3BP2 and USP10 also redistributed into SGs during PRRSV infection as they too were observed as punctate structures in the cytoplasm of infected cells. Similar to G3BP1, nearly 100% of SA-treated and PRRSV-infected cells were SG-positive for these markers while mock infected cells remained around 0%. We also observed the PRRSV-induced SGs were noticeably smaller than the SA induced SGs. Additionally the PRRSV-induced SGs also appeared to be concentrated around the nucleus, whereas the SA induced SGs had a random distribution (Fig. 1A). Western blot analysis indicated that the levels of SG markers are similar between treatment groups (Fig. 1C). To determine whether PRRSV-induced SGs are cell-specific, we also examined the distribution of G3BP1 during PRRSV infection of PK15 cells expressing the PRRSV receptor, CD163 (PK-15^{CD163}). We found that G3BP1 redistributed into SGs in PK-15^{CD163} cells and formed similar punctate structures as to the ones formed in MARC-145 cells in the cytoplasm of infected cells (Fig. 2). Collectively, these results suggest that PRRSV-induced SG formation could be a general process in response to PRRSV infection and is not cell-specific. Considering the differences is size and distribution of the PRRSV-induced SGs compared to canonical SA induced SGs, we decided to further investigate the nature of the virus-induced SGs during PRRSV infection.

3.2. SG dynamics induced in response to PRRSV infection

Several types of SGs with unique compositions have been identified to form in response to different stress conditions (Aulas et al., 2017; Yoneyama et al., 2016; Arimoto et al., 2008). However, one of the hallmark characteristics of *bona fide* SGs is the presence of mRNA (Panas et al., 2015). mRNA is thought to be temporarily stored and sequestered in SGs until resolution of the stress response (Mollet et al., 2008; Brengues et al., 2005). To determine if the PRRSV-induced SGs contain mRNA, we performed polyA mRNA fluorescent *in situ* hybridization (FISH) and co-stained for the SG marker G3BP1. As a positive control, we treated cells with SA. As expected, confocal microscopy revealed mRNA to be highly concentrated in the nucleus of all cells, but absent in the nucleolus. We also observed that both SA-treated and PRRSV-induced SGs were double positive for both G3BP1 and mRNA, while the mock-treated cells did not exhibit any SG assembly or the accumulation of mRNA into punctate cytoplasmic foci (Fig. 3A). The presence of mRNA in the PRRSV-induced SGs suggests the granules may play a role in translational regulation. Indeed, several viruses have been shown to regulate SG dynamics in order to modulate cellular protein synthesis (McCormick and Khaperskyy, 2017). To further investigate the role of the PRRSV-induced SGs during viral infection, we determined whether or not protein synthesis is indeed required for the maintenance of PRRSV-induced SGs. Here, we used cycloheximide (CHX), an inhibitor of protein translation and monitored SG dynamics using confocal microscopy and G3BP1 as a marker. CHX has been previously shown to inhibit the formation and maintenance of SGs (Panas et al., 2015). As a positive control, we monitored SGs induced by SA treatment and observed that they were disrupted when cells were incubated with CHX. Similarly, PRRSV-induced SGs were also disrupted when infected cells were incubated with CHX (Fig. 3B). These results confirm the PRRSV-induced SGs are indeed *bona fide* SGs that are both positive for mRNA and sensitive to CHX treatment. The formation of *bona fide* SGs in response to PRRSV infection suggests that they may play a functional role in regulating translation during viral replication.

3.3. PRRSV-induced SGs are associated with viral replication complexes (VRCs) and P-bodies

During the infection of some RNA viruses, SGs have been shown to redistribute around VRCs (Nikolic et al., 2016). The PRRSV NSPs have been shown to associate with viral genomic RNA to form VRCs in the cytoplasm of infected cells as sites where genome replication and

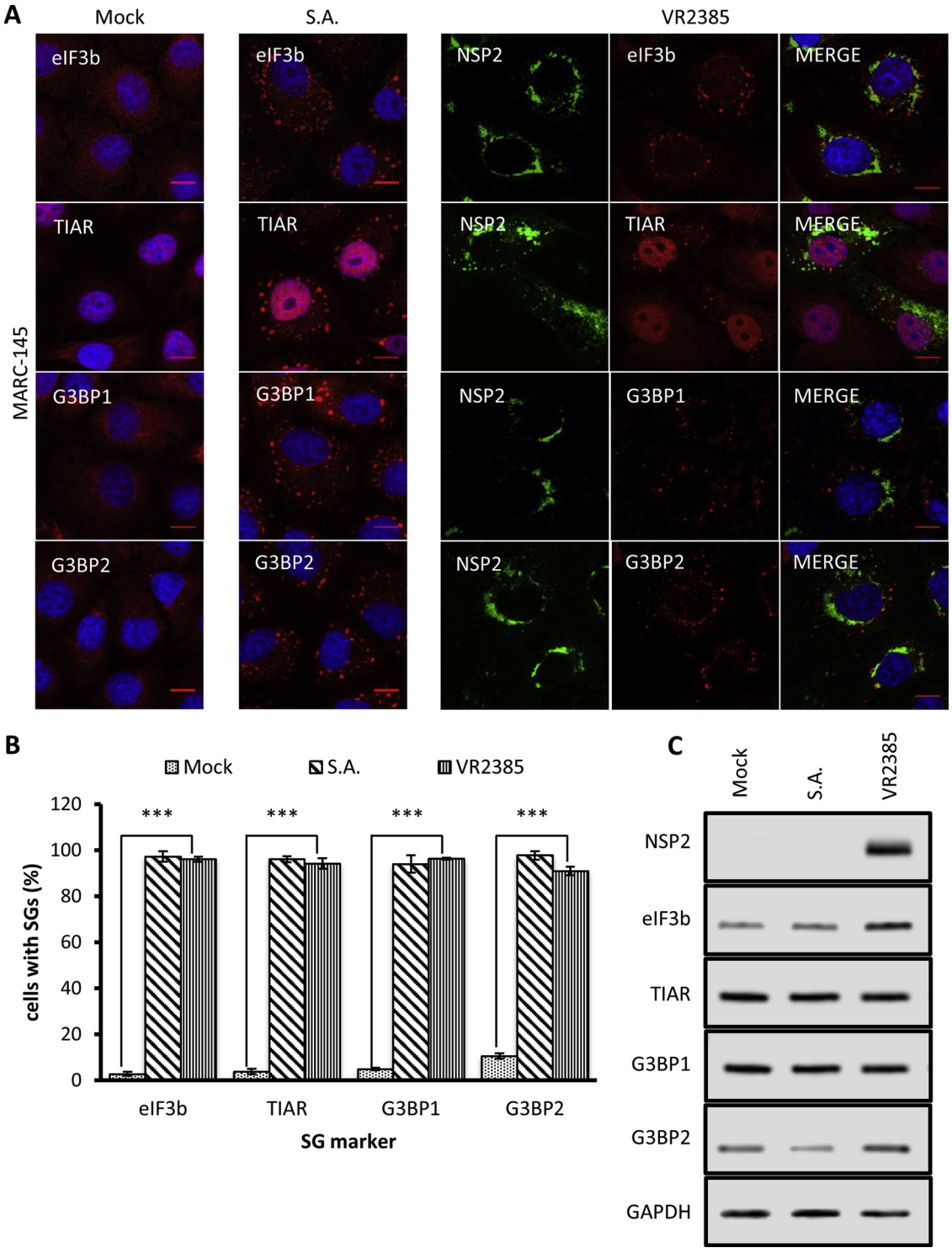

Fig. 1. PRRSV induces stress granules (SGs). **(A)**. Immunofluroescence assay (IFA) and confocal microscopy analysis of SG markers in MARC-145 cells during PRRSV infection. MARC-145 cells were mock-treated or infected with PRRSV strain VR2385 at a multiplicity of infection (MOI) of 1.0. As a positive control, cells were treated with sodium arsenite (SA, 0.5 mM) for 45 min. At 48 h post-infection (hpi), the cells were fixed and stained for the SG markers eIF3b, TIAR, G3BP1, and G3BP2. PRRSV-infected cells were identified by NSP2-EGFP. Nuclei were visualized using DAPI. Bar = 15 μM. **(B)**. Cells with SGs were quantified and presented as percentages. At least 100 cells were counted for each SG marker. Data shown are mean ± SEM and analyzed using an unpaired student's t test; ***, $P \leq 0.005$. **(C)**. Cells were treated as described in panel A, and the levels of respective SG marker proteins were examined using western blot analysis. Data is representative of 3 independent experiments.

subgenomic synthesis occurs (Fang and Snijder, 2010). To analyze the spatial distribution of SGs in relationship to PRRSV VRCs and elucidate a potential role of the PRRSV-induced SGs, we examined the localization of NSP2 and dsRNA, a viral replication intermediate and VRC marker. Both NSP2 and dsRNA are valid markers for examining VRCs during PRRSV infection (Fang and Snijder, 2010; Reid et al., 2015). As expected, confocal microscopy revealed that PRRSV NSP2 co-localized with viral dsRNA. Both NSP2 and dsRNA primarily localized around the

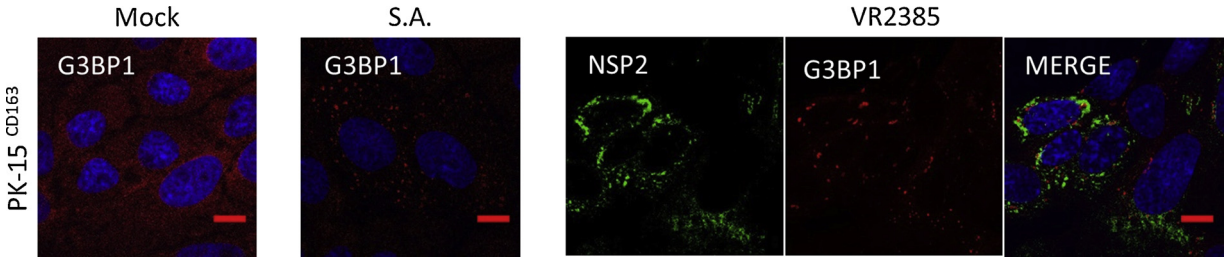

Fig. 2. PRRSV-induced SGs are not cell type-specific. Confocal microscopy analysis of SG markers in PK-15 ^{CD163} cells during PRRSV infection. PK-15 ^{CD163} cells were mock-treated or infected with PRRSV strain VR2385 at a multiplicity of infection (MOI) of 1.0. As a positive control, cells were treated with sodium arsenite (SA, 0.5 mM) for 30 min. At 48 h post-infection, the cells were fixed and stained for SGs using G3BP1 as a marker. PRRSV-infected cells were identified by NSP2-EGFP. Nuclei were visualized using DAPI.

nucleus in infected cells. Interestingly, PRRSV VRCs were shown to be in close proximity, but did not co-localize with the SG marker G3BP1 (Fig. 4A). Specifically, the PRRSV-induced SGs were observed to be located on the periphery of the VRCs and in close contact with them. Furthermore, the PRRSV-induced SGs were also juxtaposed with Dcp1a (Fig. 4B). Dcp1a is a hydrolase involved in nonsense-mediated mRNA decay pathways and is commonly used as a P-body marker (Ujwal and Parker, 2003). Collectively, our results here show that the PRRSV VRCs are associated with both SGs and P-bodies. These results suggest an interesting dynamic interplay between PRRSV replication and the mRNA storage function of the SG/P-body network.

3.4. Suppression of host cell translation coordinated with SG formation

Global repression of translation is a common strategy utilized as a host defense against cellular invaders to limit their replication (McCormick and Khaperskyy, 2017). Indeed, several viruses have been shown to activate different pathways that ultimately result in suppression of host translation (Nikolic et al., 2016; White and Lloyd, 2011; Park et al., 2008). To demonstrate that the stress response pathway of translation inhibition is activated following PRRSV infection, western blot analysis was performed to determine the phosphorylation status of eIF2a (Fig. 5A). As a positive control, SA was used to induce phosphorylation of eIF2a. As expected, SA robustly induced phosphorylation of eIF2a. Consistent with the kinetics of SG formation, PRRSV infection also significantly enhanced eIF2a phosphorylation at 48 hpi when compared to mock infected cells (Fig. 5B). Phosphorylation of eIF2a is coordinated with a global repression in translation. We therefore wanted to see if this held true during PRRSV infection. To monitor rates of cellular translation, we used puromycylation assays. Puromycin is a tRNA analogue that is incorporated into growing polypeptide chains that can be detected using a monoclonal antibody and standard immunological techniques such as immunofluorescence assays (Panas et al., 2015). When used at low concentrations for short periods of time, it is a useful diagnostic to monitor cellular translation. Using puromycylation assays coupled with confocal microscopy, we also showed that host cellular translation is dramatically reduced during PRRSV infection at this time as well (Fig. 5C). The puromycin fluorescent signal intensity was quantified using ImageJ software and used to represent *de novo* protein synthesis. As expected, PRRSV infection significantly reduced the rate of cellular translation when compared to the mock infected cells (Fig. 5D). The reduction in translation is also coordinated with the formation of SGs. G3BP1 positive SGs can be observed in PRRSV infected cells, but not in neighboring uninfected cells. More so, a visible reduction in protein synthesis can be observed in the infected cells positive for SGs. Collectively, these results suggest the PRRSV-induced SGs may play a role in regulating rates of host cellular translation during PRRSV replication. However, further experiments are warranted to fully elucidate the role of G3BP1 and G3BP2 in potentially regulating host cellular translation during PRRSV replication. Such experiments would include the monitoring of cellular translation using the puromycylation assay under silencing of G3BP1, G3BP2 and G3BP1/2 under during S.A. treatment as well as VR2385 infection.

3.5. G3BP1 and G3BP2 are not required for PRRSV replication

The SG components G3BP1 and G3BP2 have been shown to be necessary for SG assembly (Tourrière et al., 2003). To determine if SGs are necessary for efficient PRRSV replication, we first generated MARC-145 stable cell lines in which the expression of G3BP1 and G3BP2 were knocked down. Knock down efficiency was determined using western blot analysis with antibodies that specifically recognize G3BP1 and G3BP2 (Fig. 6A). The levels of G3BP1 and G3BP2 were then quantified and normalized to GAPDH using Licor ImageStudio software (Fig. 6B). An approximate 70% and 80% reduction in G3BP1 and G3BP2, respectively can be observed in cells in which the proteins were individually knocked down. For double knock downs, an approximate 40% and 30% reduction in G3BP1 and G3BP2 was observed. The cells were then subsequently infected with PRRSV and the kinetics of viral replication were determined using plaque assays (Fig. 6C). The results showed that knocking down G3BP1 and G3BP2 individually or together had no effect on viral replication, suggesting that SGs are not important for efficient viral replication. In addition, we also determined that knocking down USP10 also did not affect viral replication (Supplemental Fig. S1).

4. Discussion

The main function of SGs is to prevent apoptosis and promote cellular survival during times of stress such as virus infections (Arimoto et al., 2008; McCormick and Khaperskyy, 2017). This is accomplished by regulating rates of host cellular translation. However, SGs have been recently determined to play alternative and unique roles during viral infection. In the case of certain RNA viruses, such as West Nile virus and Dengue virus, SG components play important proviral roles during viral infections. G3BP1 binds to and stabilizes viral RNAs to prevent degradation (Bidet et al., 2014; Li et al., 2002). Conversely, in the cases of poliovirus and hepatitis C virus, SGs have been shown to act as antiviral signaling platforms to initiate innate immune responses (Garaigorta et al., 2012; Onomoto et al., 2012). In this situation, proteases encoded by the viral genome cleave G3BP1 to prevent SG formation and subsequent antiviral signaling pathways (Garaigorta et al., 2012; Beckham and Parker, 2008). The mechanisms by which viruses subvert or hijack the SG machinery are still not fully understood. A more thorough understanding of the molecular mechanisms involving SG formation and dynamics during viral infection will help understand the mechanisms of viral pathogenesis.

While PRRSV has been recently shown to induce SGs, the exact nature of SG formation and its underlying mechanism of regulating antiviral immune response during PRRSV infection remain unclear (Zhou et al., 2017). Formation of PRRSV-induced SGs was observed in

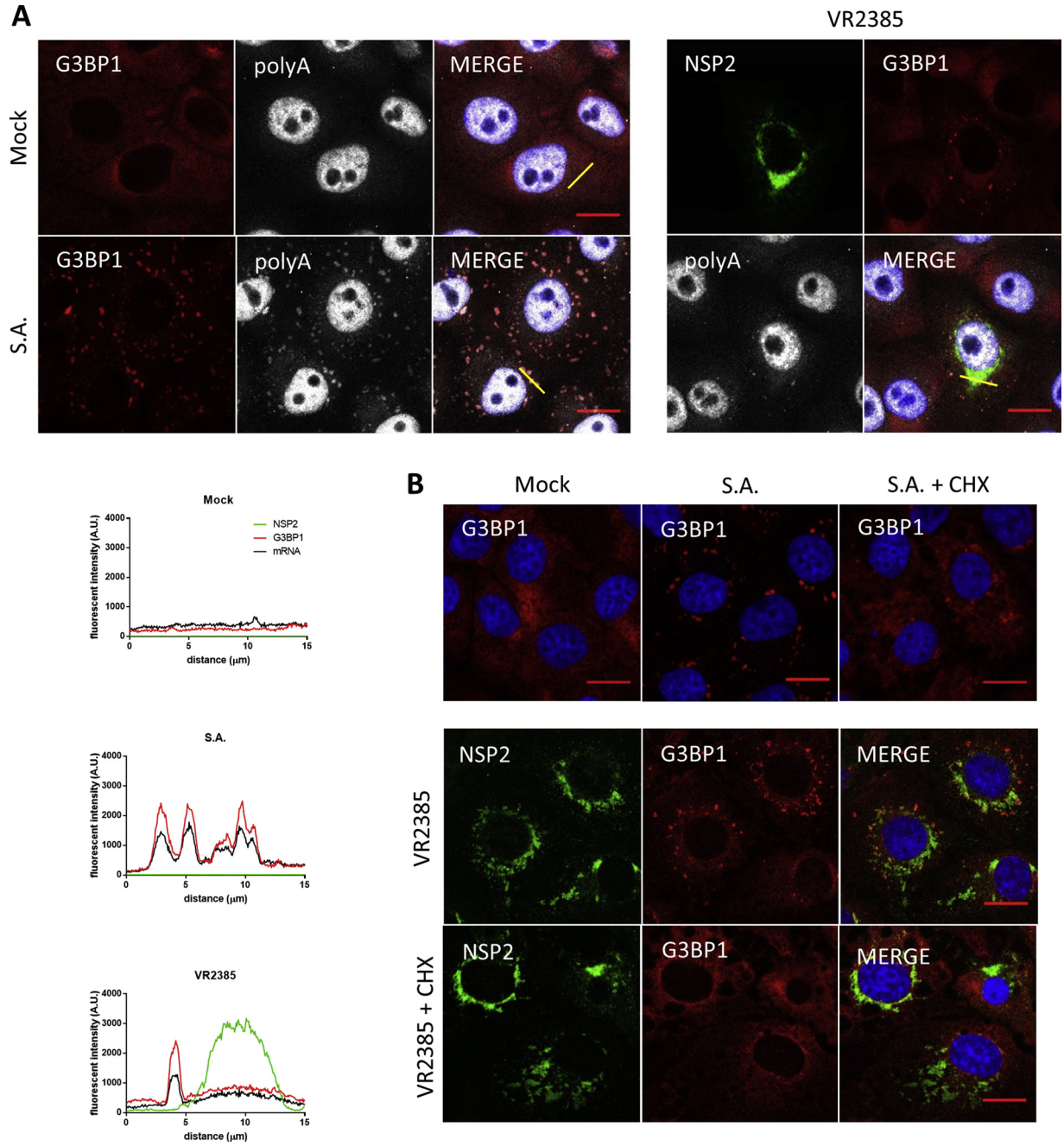

Fig. 3. PRRSV-induced SGs are *bona fide* SGs. **(A)**. Confocal microscopy analysis of SGs and mRNA in MARC-145 cells during PRRSV infection. MARC-145 cells were mock-treated or infected with PRRSV strain VR2385 at a multiplicity of infection (MOI) of 1.0. As a positive control, cells were treated with sodium arsenite (SA, 0.5 mM) for 45 min. At 48 h post-infection, the cells were fixed and co-stained for SGs using G3BP1 as a marker and polyA *in situ* hybridization of mRNA. PRRSV-infected cells were identified by NSP2-EGFP. Nuclei were visualized using DAPI. Bar = 15 μM. **(B)**. Cells were treated as described in panel A. At 48 h post-infection, cells were incubated with cycloheximide (CHX, 50 μM) for 3 h. After CHX treatment, cells were then fixed and stained for SGs using G3BP1 as a marker. PRRSV-infected cells were identified by NSP2-EGFP. Nuclei were visualized using DAPI. Bar = 15 μM. Intensity plots represent the fluorescent intensity and co-localization of green, red and grey pixels along the yellow line drawn in the merged channel.

MARC145 cells (Chen et al., 2018) and PAM cells (Zhou et al., 2017). However, previous work in PAM cells is very limited, as only a single SG marker (TIAR) was used. Since SGs are very diverse in composition and function, the structures reported by Chen et al cannot be concluded as indeed *bona fide* SGs without the use of additional markers and assays. Therefore, it is critically important to more extensively investigate the formation and underlying mechanism of PRRSV-induced SGs.

In this present study, we further delineated these mechanisms involved in PRRSV-induced SG formation. Using confocal microscopy, we determined the cellular components involved in formation of PRRSV-induced SGs. We found that eIF3b, TIAR, G3BP1 and G3BP2 are major components of PRRSV-induced SGs in MARC-145 and PK-15-CD163 cells, suggesting that the PRRSV-induced SG response is not cell type-specific and could be a general response to PRRSV infection.

The formation of SGs in response to PRRSV infection appears to be dependent on PERK-mediated eIF2a phosphorylation. The eIF2a pathway is a critical regulator of cellular translation in response to various stress conditions. PERK is one of 4 known eIF2a kinases that respond to cellular stress and is activated upon ER stress. Such stress can be triggered by an overload of unfolded proteins in the ER, as

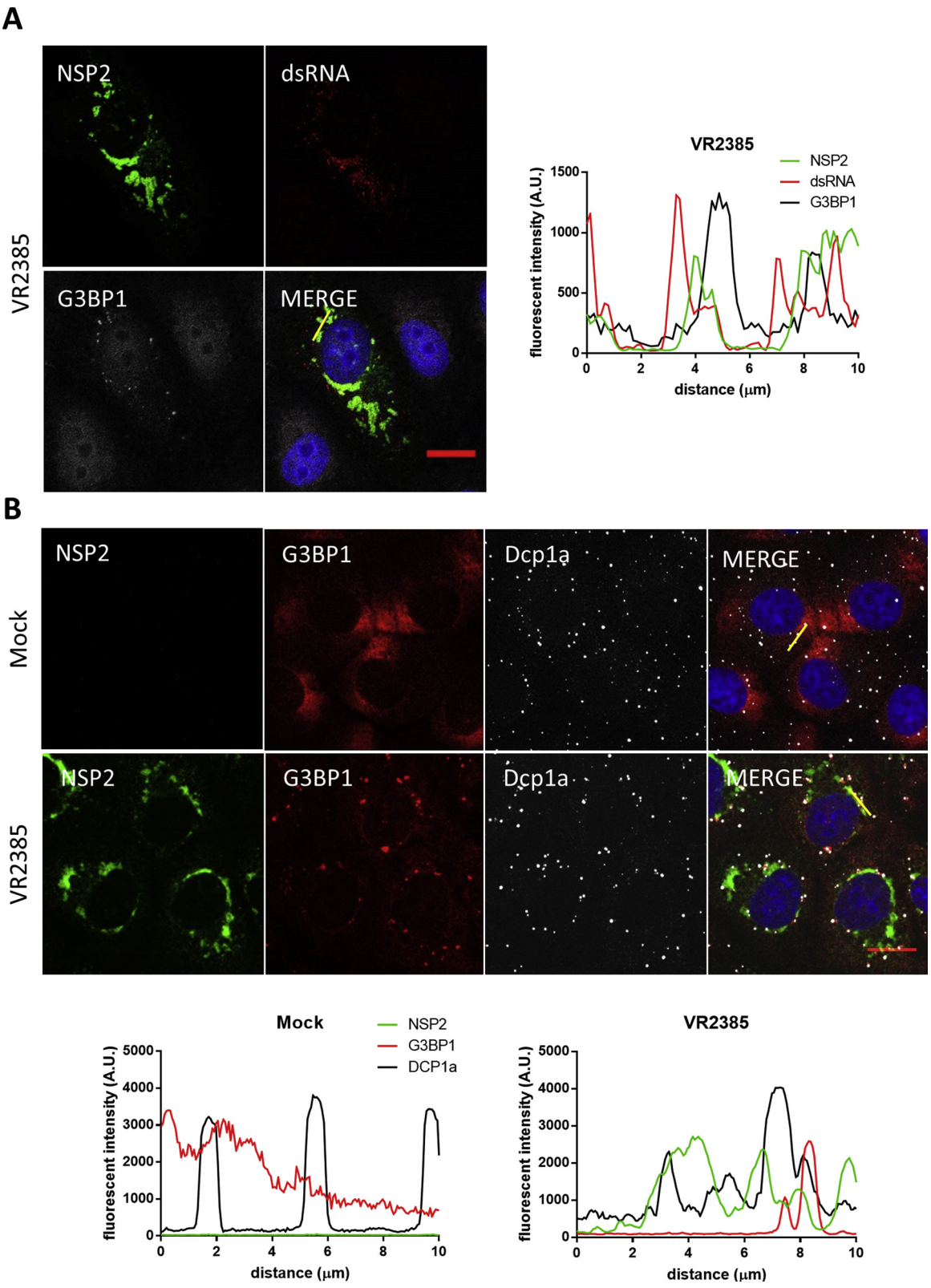

Fig. 4. PRRSV-induced SGs are closely associated with viral replication complex (VRCs) and P-bodies. **(A)**. Confocal microscopy analysis of SG markers in MARC-145 cells during PRRSV infection. MARC-145 cells were mock-treated or infected with PRRSV strain VR2385 at a multiplicity of infection (MOI) of 1.0. At 48 h post-infection, the cells were then fixed and co-stained for the SG marker G3BP1 and VRC marker dsRNA. PRRSV-infected cells were identified by NSP2-EGFP. Nuclei were visualized using DAPI. Bar = 15 μM. **(B)**. Cells were treated as described in panel A. At 48 h post-infection, cells were fixed and co-stained for the SG marker G3BP1 and P-body marker Dcp1a. PRRSV-infected cells were identified by NSP2-EGFP. Nuclei were visualized using DAPI. Bar = 15 μM. Intensity plots represent the fluorescent intensity and co-localization of green, red and grey pixels along the yellow line drawn in the merged channel in both panels A and B.

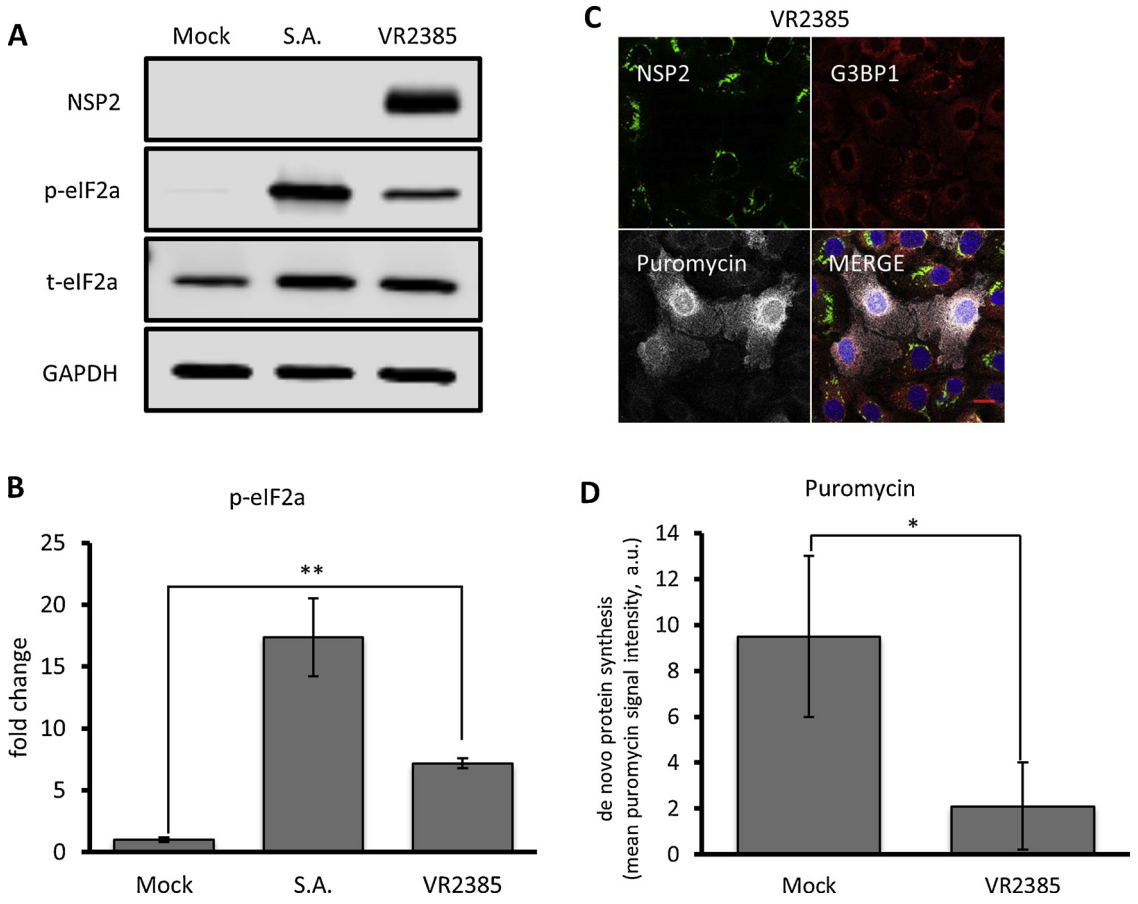

Fig. 5. PRRSV-induced SGs are coordinated with suppression of global host cell translation. **(A)**. Western blot analysis of eIF2a phosphorylation status during PRRSV infection. MARC-145 cells were mock-treated or infected with PRRSV strain VR2385 at a multiplicity of infection (MOI) of 1.0. As a positive control, cells were treated with sodium arsenite (SA, 0.5 mM) for 45 min. At 48 h post-infection, the cells were then harvested for western blot analysis of phosphorylated eIF2a. **(B)**. Proteins were quantified from western blot using densitometry analysis and normalized to GAPDH. Fold change of SA and VR2385 verses mock were plotted. Data shown are mean ± SEM and analyzed using an unpaired student's t test; **P ≤ 0.005. Data is representative of 3 independent experiments. **(C)**. Cells were treated as described in panel A. At 48 h post-infection, cells were incubated with puromycin (10 u M) for 15 min. After puromycin treatment, cells were fixed and stained with a puromycin antibody to visualize protein synthesis. PRRSV-infected cells were identified by NSP2-EGFP. Nuclei were visualized using DAPI. Bar = 15 μM. **(D)**. The rate of *de novo* protein synthesis was quantified by measuring puromycin fluorescent signal intensity using ImageJ software. At least 100 cells were counted for each treatment group. Data shown are mean ± SEM and analyzed using an unpaired student's t test; *, P ≤ 0.05.

occurs during infection of most viruses. Treatment of cells with PERK inhibitor prevents eIF2a phosphorylation and subsequent SG formation in PRRSV infected cells (Zhou et al., 2017). PRRSV could potentially be using the eIF2a pathway to its advantage in order to facilitate viral replication. A reduction in global translation could result into a reduction in overall antiviral signaling, thus creating a favorable environment suitable for replication. Additional work is therefore warranted in the future to determine the true nature of the PRRSV-induced SGs and the pathways involved in their formation.

Importantly, FISH analysis and confocal microscopy revealed that mRNA, a hallmark characteristic of functional *bona fide* SGs, is also recruited to the PRRSV-induced SGs. Considering the composition of the PRRSV-induced SGs as well as the fact that their disassembly is facilitated by CHX, we conclude that the PRRSV-induced SGs are *bona fide* SGs. Indeed, the finding that mRNA is recruited to the PRRSV-induced SGs suggests that they may be acting as a storage repository for RNA transcripts.

While SGs have been shown to temporarily store mRNAs until resolution of stress conditions and granule disassembly, the exact fate of these transcripts is not fully understood (Panas et al., 2016). It is currently thought that RNA transcripts retained in SGs are released back into the cytoplasm for subsequent translation and protein synthesis. Alternatively, if stress is not resolved, the transcripts could be shuttled to P-bodies instead (Mollet et al., 2008; Brengues et al., 2005). In this study, we found that the PRRSV induced SGs are closely associated with P-bodies and VRCs. The SG marker G3BP1 and P-body marker Dcp1a were found to be in close proximity to the sites of PRRSV replication, as indicated by the presence of the viral protease, NSP2. These data suggest that mRNA is potentially stored and transferred between these sites during PRRSV infection. Moreover, we show that the rate of host cellular protein synthesis is drastically reduced during PRRSV infection. Importantly, we demonstrated that this reduction of protein synthesis is coordinated with SG formation during PRRSV infection. Taken together, these data suggest a possible mechanism in which the PRRSV-induced SGs function to sequester mRNAs and preclude them from being translated. Alternatively, this data also suggests that the PRRSV-induced SGs could also play an important role in regulating the PRRSV lifecycle and facilitate the switch from genome translation to replication.

While other viruses have been shown to utilize SG components to enhance their replication and carry out infection, SGs seem to be dispensable for PRRSV replication. In this study, we used shRNAs to knock down both G3BP1 and G3BP2 individually and together and observed no difference in PRRSV replication as determined by plaque assay. However, additional parameters need to be investigated in the future before any definitive conclusions are made. Specifically, the role of SGs in disease pathogenesis warrants further investigation, as their function in regulating the expression of specific cytokines during PRRSV

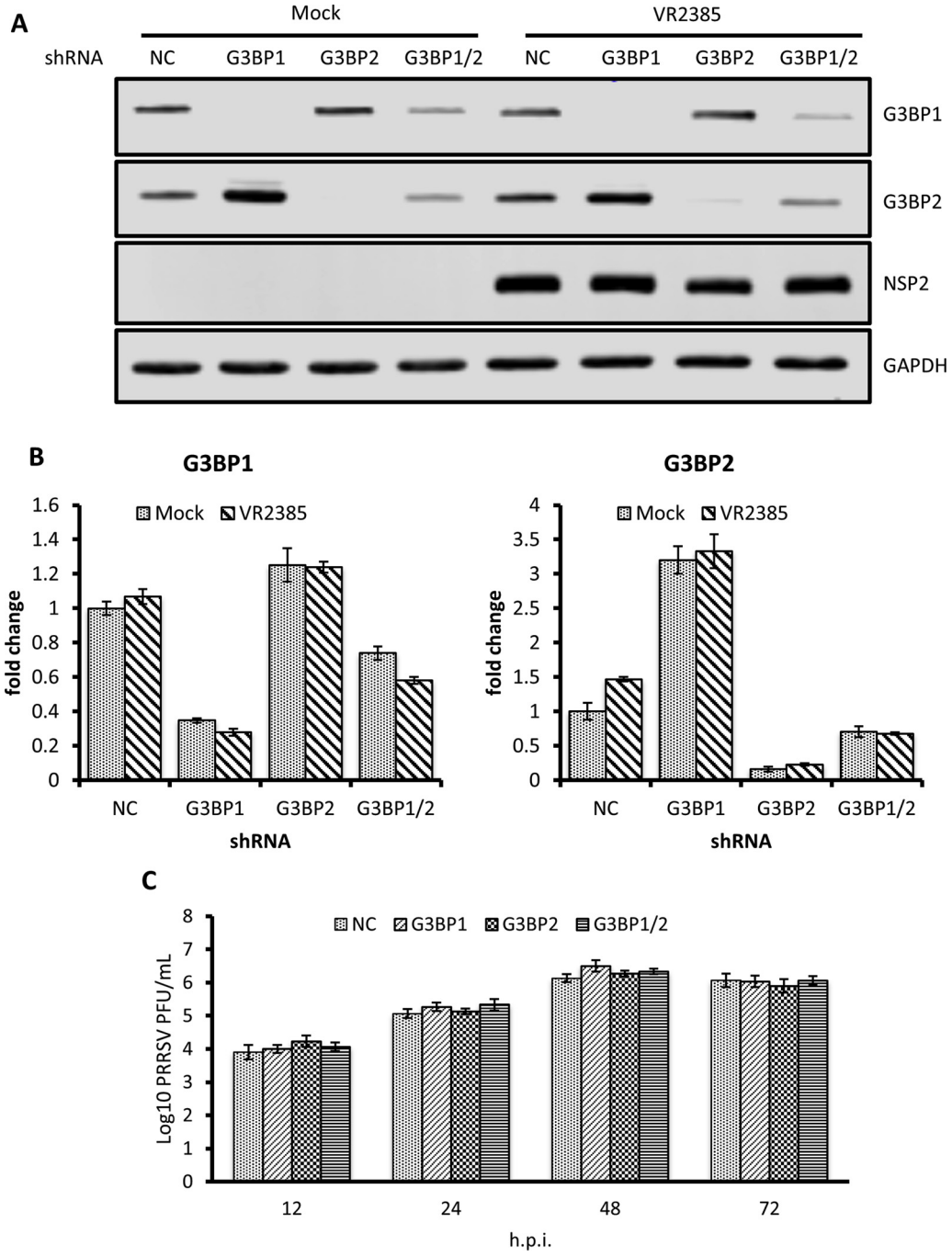

Fig. 6. G3BP1 and G3BP2 are not required for PRRSV replication. **(A)**. Western blot analysis of shRNA knock-down of G3BP1, G3BP2 or both (G3BP1/2) in mock- and PRRSV-infected MARC-145 cells. At 48 h post-infection, the infected cells were harvested for western blot analysis of G3BP1, G3BP2 and NSP2. **(B)**. Quantification of G3BP1 and G3BP2 protein levels normalized to GAPDH. Cells were treated as described in panel A and the levels of respective protein were measured using ImageStudio software. Data shown are mean ± SEM and representative of 3 independent experiments. **(C)**. Effect of G3BP1 and G3BP2 knock-down on PRRSV replication. Cells were treated as described in panel A and the infectious virus titers from culture supernatants were determined using plaque assays. Data shown are mean ± SEM and analyzed using an unpaired student's *t*-test Data is representative of 3 independent experiments.

infection has yet to be fully elucidated. Interestingly, when G3BP1 and G3BP2 were knocked down individually, we observed a strong up-regulation of the other protein (Fig. 6A). When both proteins were knocked down together, we observed a weaker reduction in both proteins compared to individual knock-downs. One potential explanation for this observation is a form of genetic compensation: when one protein is reduced, the cell up-regulates expression of another related protein to compensate for the loss.

In conclusion, we provide convincing evidence that the PRRSV-induced SGs are indeed *bona fide* SGs. While we determined that mRNA is present in the PRRSV-induced SGs, we did not distinguish its origin. Future studies will need to determine whether the mRNA stored in PRRSV-induced SGs is of cellular or viral origin. It is interesting to speculate that specific RNA transcripts are recruited to the PRRSV-induced SGs in order to regulate translation of either host or viral mRNAs. We also identified the SG components G3BP1, G3BP2 and USP10 are dispensable for PRRSV replication. Ultimately, our data suggests that the PRRSV-induced SGs may function to suppress host cellular translation, however, further experiments are needed to definitively support this hypothesis. Indeed, monitoring puromycylation under G3BP1/2 knock-down condition in the context of PRRSV infection would inform whether the PRRSV-induced SGs regulate host cellular translation. Furthermore, the fate of RNA transcripts sequestered in the PRRSV-induced SGs remains to be determined. There are many important but unanswered questions that are beyond the scope of this initial study. For example, are the transcripts being stored temporarily in SGs, or transferred to P-bodies for degradation? Are specific transcripts recruited to SGs during PRRSV infection? A better understanding of the molecular events involved in the formation of PRRSV-induced SGs will undoubtedly help understand the molecular mechanism of PRRSV

pathogenesis.

Conflict of interest

The authors declare they have no conflicts of interest regarding the contents of this study.

Acknowledgements

This work was supported by a pre-doctorial fellowship grant to Nicholas Catanzaro from the U.S. Department of Agriculture National Institute of Food and Agriculture (USDA NIFA 2017-67011-26045). The authors thank the expert assistance of C. Lynn Heffron, Shannon Matzinger, Sakthivel Subramaniam, Debin Tian, and Qian Cao for their help and guidance with this work.

Appendix A. Supplementary data

Supplementary material related to this article can be found, in the online version, at doi:https://doi.org/10.1016/j.virusres.2019.02.016.

References

Arimoto, K., Fukuda, H., Imajoh-Ohmi, S., Saito, H., Takekawa, M., 2008. Formation of stress granules inhibits apoptosis by suppressing stress-responsive MAPK pathways. Nat. Cell Biol. 10, 1324–1332.
Aulas, A., Fay, M.M., Lyons, S.M., Achorn, C.A., Kedersha, N., Anderson, P., Ivanov, P., 2017. Stress-specific differences in assembly and composition of stress granules and related foci. J. Cell. Sci. 130, 927–937.
Beckham, C.J., Parker, R., 2008. P bodies, stress granules, and viral life cycles. Cell Host Microbe 3, 206–212.
Beura, L.K., Sarkar, S.N., Kwon, B., Subramaniam, S., Jones, C., Pattnaik, A.K., Osorio, F.A., 2010. Porcine reproductive and respiratory syndrome virus nonstructural protein 1 modulates host innate immune response by antagonizing IRF3 activation. J. Virol. 84, 1574–1584.
Beura, L.K., Subramaniam, S., Vu, H.L.X., Kwon, B., Pattnaik, A.K., Osorio, F.A., 2012. Identification of amino acid residues important for anti-IFN activity of porcine reproductive and respiratory syndrome virus non-structural protein 1. Virology 433, 431–439.
Bidet, K., Dadlani, D., Garcia-Blanco, M.A., 2014. G3BP1, G3BP2 and CAPRIN1 are required for translation of interferon stimulated mRNAs and are targeted by a dengue virus non-coding RNA. PLoS Pathog. 10, e1004242.
Brengues, M., Teixeira, D., Parker, R., 2005. Movement of eukaryotic mRNAs between polysomes and cytoplasmic processing bodies. Science 310, 486–489.
Chen, W.-Y., Schniztlein, W.M., Calzada-Nova, G., Zuckermann, F.A., 2018. Genotype 2 strains of porcine reproductive and respiratory syndrome virus dysregulate alveolar macrophage cytokine production via the unfolded protein response. J. Virol. 92.
Collins, J.E., Benfield, D.A., Christianson, W.T., Harris, L., Hennings, J.C., Shaw, D.P., Goyal, S.M., McCullough, S., Morrison, R.B., Joo, H.S., 1992. Isolation of swine infertility and respiratory syndrome virus (isolate ATCC VR-2332) in North America and experimental reproduction of the disease in gnotobiotic pigs. J. Vet. Diagn. Invest. 4, 117–126.
Fang, Y., Snijder, E.J., 2010. The PRRSV replicase: Exploring the multifunctionality of an intriguing set of nonstructural proteins. Virus Res. 154, 61–76.
Garaigorta, U., Heim, M.H., Boyd, B., Wieland, S., Chisari, F.V., 2012. Hepatitis C virus (HCV) induces formation of stress granules whose proteins regulate HCV RNA replication and virus assembly and egress. J. Virol. 86, 11043–11056.
Holtkamp, D., Kliebenstein, J., Neumann, E., Zimmerman, J., Rotto, H., Yoder, T., Wang, C., Yeske, P., Mowrer, C., Haley, C., 2013. Assessment of the economic impact of porcine reproductive and respiratory syndrome virus on United States pork producers. J. Swine Health Prod. 21, 72–84.
Ke, H., Yoo, D., 2017. The viral innate immune antagonism and an alternative vaccine design for PRRS virus. Vet. Microbiol. 209, 75–89.
Kedersha, N.L., Gupta, M., Li, W., Miller, I., Anderson, P., 1999. RNA-binding proteins Tia-1 and Tiar link the phosphorylation of Eif-2α to the assembly of mammalian stress granules. J. Cell Biol. 147, 1431–1442.
Li, W., Li, Y., Kedersha, N., Anderson, P., Emara, M., Swiderek, K.M., Moreno, G.T., Brinton, M.A., 2002. Cell proteins TIA-1 and TIAR interact with the 3' stem-loop of the West Nile virus complementary minus-strand RNA and facilitate virus replication. J. Virol. 76, 11989–12000.
Lloyd, R.E., 2012. How Do Viruses Interact with Stress-Associated RNA Granules? PLoS Pathog. 8, e1002741.
Lunney, J.K., Benfield, D.A., Rowland, R.R.R., 2010. Porcine reproductive and respiratory syndrome virus: an update on an emerging and re-emerging viral disease of swine. Virus Res. 154, 1–6.
McCormick, C., Khaperskyy, D.A., 2017. Translation inhibition and stress granules in the antiviral immune response. Nat. Rev. Immunol. 17, 647–660.
Meng, X.-J., Paul, P.S., Halbur, P.G., 1994. Molecular cloning and nucleotide sequencing of the 3′-terminal genomic RNA of the porcine reproductive and respiratory syndrome virus. J. Gen. Virol. 75, 1795–1801.
Meng, X.-J., Paul, P.S., Morozov, I., Halbur, P.G., 1996. A nested set of six or seven subgenomic mRNAs is formed in cells infected with different isolates of porcine reproductive and respiratory syndrome virus. J. Gen. Virol. 77, 1265–1270.
Meulenberg, J.M., Hulst, M.M., Meijer, E.J., PLJM, Moonen, Moormann, R.J.M., 1993. Lelystad virus, the causative agent of porcine epidemic abortion and respiratory syndrome (PEARS), is related to LDV and EAV. Virology 192, 62–72.
Mollet, S., Cougot, N., Wilczynska, A., Dautry, F., Kress, M., Bertrand, E., Weil, D., 2008. Translationally repressed mRNA transiently cycles through stress granules during stress. Mol. Biol. Cell 19, 4469–4479.
Neumann, E.J., Kliebenstein, J.B., Johnson, C.D., Mabry, J.W., Bush, E.J., Seitzinger, A.H., Green, A.L., Zimmerman, J.J., 2005. Assessment of the economic impact of porcine reproductive and respiratory syndrome on swine production in the United States. J. Am. Vet. Med. Assoc. 227, 385–392.
Ni, Y.-Y., Huang, Y.-W., Cao, D., Opriessnig, T., Meng, X.-J., 2011. Establishment of a DNA-launched infectious clone for a highly pneumovirulent strain of type 2 porcine reproductive and respiratory syndrome virus: Identification and in vitro and in vivo characterization of a large spontaneous deletion in the nsp2 region. Virus Res. 160, 264–273.
Nikolic, J., Civas, A., Lama, Z., Lagaudrière-Gesbert, C., Blondel, D., 2016. Rabies virus infection induces the formation of stress granules closely connected to the viral factories. PLoS Pathog. 12, e1005942.
Onomoto, K., Jogi, M., Yoo, J.-S., Narita, R., Morimoto, S., Takemura, A., Sambhara, S., Kawaguchi, A., Osari, S., Nagata, K., Matsumiya, T., Namiki, H., Yoneyama, M., Fujita, T., 2012. Critical role of an antiviral stress granule containing RIG-I and PKR in viral detection and innate immunity. PLoS One 7, e43031.
Panas, M.D., Kedersha, N., McInerney, G.M., 2015. Methods for the characterization of stress granules in virus infected cells. Methods 90, 57–64.
Panas, M.D., Ivanov, P., Anderson, P., 2016. Mechanistic insights into mammalian stress granule dynamics. J. Cell Biol. 215, 313–323.
Park, N., Katikaneni, P., Skern, T., Gustin, K.E., 2008. Differential targeting of nuclear pore complex proteins in poliovirus-infected cells. J. Virol. 82, 1647–1655.
Reid, C., Airo, A., Hobman, T., 2015. The virus-host interplay: biogenesis of +RNA replication complexes. Viruses 7, 4385–4413.
Renukaradhya, G.J., Meng, X.-J., Calvert, J.G., Roof, M., Lager, K.M., 2015. Live porcine reproductive and respiratory syndrome virus vaccines: current status and future direction. Vaccine 33, 4069–4080.
Snijder, E.J., Kikkert, M., Fang, Y., 2013. Arterivirus molecular biology and pathogenesis. J. Gen. Virol. 94, 2141–2163.
Sun, Y., Han, M., Kim, C., Calvert, J.G., Yoo, D., 2012a. Interplay between interferon-mediated innate immunity and porcine reproductive and respiratory syndrome virus. Viruses 4, 424–446.
Sun, Z., Li, Y., Ransburgh, R., Snijder, E.J., Fang, Y., 2012b. Nonstructural protein 2 of porcine reproductive and respiratory syndrome virus inhibits the antiviral function of interferon-stimulated gene 15. J. Virol. 86, 3839–3850.
Taniuchi, S., Miyake, M., Tsugawa, K., Oyadomari, M., Oyadomari, S., 2016. Integrated stress response of vertebrates is regulated by four eIF2α kinases. Sci. Rep. 6.
Tourrière, H., Chebli, K., Zekri, L., Courselaud, B., Blanchard, J.M., Bertrand, E., Tazi, J., 2003. The RasGAP-associated endoribonuclease G3BP assembles stress granules. J. Cell Biol. 160, 823–831.
Ujwal, S., Parker, R., 2003. Decapping and decay of messenger RNA occur in cytoplasmic processing bodies. Science 300, 805–808.
White, J.P., Lloyd, R.E., 2011. Poliovirus unlinks TIA1 aggregation and mRNA stress granule formation. J. Virol. 85, 12442–12454.
Yoneyama, M., Jogi, M., Onomoto, K., 2016. Regulation of antiviral innate immune signaling by stress-induced RNA granules. J. Biochem. (Tokyo) 279–286.
Zhou, Y., Fang, L., Wang, D., Cai, K., Chen, H., Xiao, S., 2017. Porcine reproductive and respiratory syndrome virus infection induces stress granule formation depending on protein kinase R-like endoplasmic reticulum kinase (PERK) in MARC-145 cells. Front. Cell. Infect. Microbiol. 7.